

Optimal Design of a Medical Robot for Minimally Invasive Surgery

Rainer Konietschke^{*,1}, Tobias Ortmaier¹, Holger Weiss¹,
Robert Engelke², and Gerd Hirzinger¹

¹*German Aerospace Center, Institute of Robotics
and Mechatronics, P.O. Box 1116,
D-82230 Weßling, Germany*

²*Munich University of Technology, Institute of
Applied Mechanics, D-85747 Garching, Germany*

Abstract. This paper presents a framework for the optimisation of the design of a medical robot to accomplish minimally invasive surgery. Surgical interventions are analysed in terms of workspace and accuracy requirements. As optimisation criterion, the minimisation of the overall size of the robot is considered since a compact design is important in an overcrowded environment such as the operating room. Stress is laid on the formulation of reasonable measures for manipulability and accuracy which are included in the optimisation model as constraints. Furthermore, a method to allow for insensitive robot setups with respect to registration errors is established. Optimisation itself is carried out using genetic algorithms with a subsequent gradient-based method. As a result, the optimal link lengths of a medical robot are determined.

Keywords: accuracy, manipulability, robotic assistance, minimally invasive surgery, optimisation, robot design, genetic algorithms

1 Introduction

The use of tele-operated systems for minimally invasive surgery (MIS) such as the daVinciTM or ZEUSTM robot systems has been investigated closely in the last few years. The diversity of surgical interventions carried out or proposed to be carried out with robotic assistance increases constantly. In this context, the optimal design of a robot with respect to its envisioned surgical interventions is of

special interest. Until now, to the authors' knowledge there are no guidelines for optimal robot design in the field of robotically assisted MIS available.

For an advanced robotic system for thoracic surgery, the following questions are important:

1. Fields of application: What surgical interventions shall be carried out with the robot and how can these interventions be formulated mathematically?
2. Optimisation criteria and constraints: Given different robot setups¹, which of them is the best?
3. Optimisation method: Which optimisation method is suited best to solve the optimisation problem?

Related work in preoperative planning of robotically assisted MIS [1, 3, 5, 8, 11, 13] does not take into account measures such as manipulability and accuracy. Instead, the following approaches are used: Tool dexterity [1, 8] as well as the magic pyramid [3] evaluate the orientation of the instruments, the endoscope, and the surface normal of the considered operating field to each other. [5] considers the distance of the joint angles of the robot from its maximum values.

Experimental trials [1] suggest the conclusion that the use of more sophisticated descriptions of manipulability and accuracy measures is reasonable. Potential advantages are:

- No occurrence of singular configurations which could cause system failures.

¹In this paper, the “setup” of the robot is defined to comprise the link lengths of the robot as well as terms specific to each surgical intervention considered, like the position of the robot and the position of the entry point into the human body.

*Rainer.Konietschke@dlr.de

- A certain minimal velocity of the instrument tip both in terms of translation and rotation can be realised all over the considered operating field. This is important to assure that motions commanded by the surgeon can be performed by the robot system.
- The demanded accuracy of the positioning of the instrument tip can be guaranteed. This is of great interest if very fine structures (e.g. blood vessels) are manipulated.

Therefore, the focus of this work is laid on the formulation of significant measures for manipulability and accuracy.

In the next section, the underlying problem is described. Section 3 summarises how the optimisation is realised and in Sect. 4 the results are discussed.

2 Problem Statement

In this section, the kinematics of the considered robot and the optimisation parameters are described.

Kinematics. A robot with 6 degrees of freedom (DoFs) as shown in Fig. 1 is considered. Two additional DoFs (Θ_7 and Θ_8) are added if an actuated instrument is used. Taking into account the loss of 2 DoFs due to kinematic restrictions at the entry point into the human body, full 6 DoFs remain for the manipulation of the instrument tip if an actuated instrument is attached to the robot. Using a rigid instrument, only translation in all three directions and rotation around the instrument axis Θ_6 can be realised.²

Dynamics are not included in the modelling since typical motions in MIS are too small to induce significant forces. Furthermore, a single-robot setup without collision detection is considered. The aspects of a multi-robot setup with collision detection will be subject to future work (see Sect. 5).

Optimisation Parameters. The aim of the optimisation algorithm is to find the optimal link lengths l_1 and l_2 as depicted in Fig. 1. Additionally, the position of the robot base (addressed by its distance from the center of the operating field l_x and its height of mounting l_h) and the length of

²The notation Θ_i stands both for the joint i and the axis direction parallel to the rotation axis of that same joint.

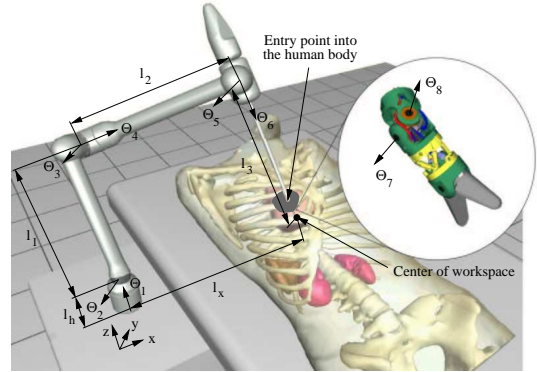


Figure 1: Surgical robot and actuated instrument tip.

the instrument l_3 are included as optimisation parameters (see Fig 1). In this context it has to be mentioned that it is not intended to solve a robot positioning problem. However, since the positioning parameters l_x and l_h have a big influence on the optimal link lengths, these parameters cannot be fixed preliminarily. The instrument length l_3 is planned to be variable according to the intervention. Due to the leverage effect in connection with the entry point into the human body, the instrument length l_3 has a strong influence on the chosen formulations of manipulability and accuracy and therefore plays an important role in determining the optimal link lengths of the robot.

3 Methods

The optimal link lengths of the robot are determined in three steps: The considered surgical interventions are analysed in terms of workspace and demanded positioning accuracy (Sect. 3.1), the optimisation criterion and the constraints are defined (Sect. 3.2), and a suitable optimisation method is chosen (Sect. 3.3).

3.1 Surgical Interventions

The following interventions are taken into account:

- Cardiac interventions:
 - Totally endoscopic bypass graft
 - Mitral/aortic valve repair/replacement
 - Tricuspid valve repair

- Abdominal interventions:
 - Cholecystectomy
 - Appendectomy
 - Hernia repair
 - Laparoscopy

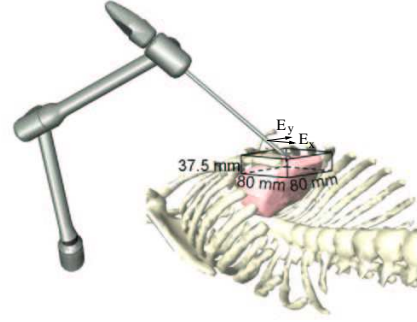
The analysis of the above mentioned interventions yields the three workspaces shown in Fig. 2: The standard workspace includes all considered interventions with actuated instruments except for the left internal mammary artery (LIMA) takedown. As can be seen in Fig. 2(b), this specific intervention requires a distinctively different robot setup because the position of the entry point into the human body is lateral. Surgical interventions with non-actuated instruments are analysed by the third workspace.

In contrast to preoperative planning, where only one specific patient geometry is of interest, these workspaces comprise representative patient geometries obtained from analysing different patients. Therefore, the workspaces are larger than actually necessary when only one specific case is considered, but on the other hand it can be guaranteed that the robot is suitable for various patient geometries.

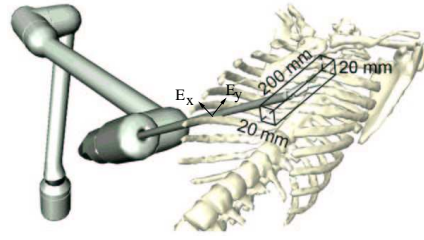
Concerning the accuracy that is necessary to perform the considered tasks, the anastomosis was identified to be most demanding. The stitches have a mean distance of $d = 0.5$ mm to each other. Thus, a necessary translational positioning accuracy of $\Delta x_{\min} = 0.1$ mm is assumed. This value corresponds to the positioning accuracy that a surgeon with visual feedback can achieve as measured in [10, 12, 6]. No publications are known to the author that analyse rotational accuracies or appearing velocities in surgical interventions. In this work, a rotational accuracy of $\Delta \alpha_{\min} = 0.5^\circ$, and velocities of $\dot{x}_{\min} = 60 \frac{\text{mm}}{\text{s}}$ for translation and $\dot{\alpha}_{\min} = 30^\circ \text{s}^{-1}$ for rotation are assumed (see Table 1 for these constraints and the parameters predetermined from design).

Maximum joint velocity $\dot{\Theta}_{\text{MAX}}$	225°s^{-1}
Resolution of decoders $\Delta \Theta_{\min}$	0.001°
Translational velocity \dot{x}_{\min}	$60 \frac{\text{mm}}{\text{s}}$
Translational accuracy Δx_{\min}	0.1 mm
Rotational velocity $\dot{\alpha}_{\min}$	30°s^{-1}
Rotational accuracy $\Delta \alpha_{\min}$	0.5°

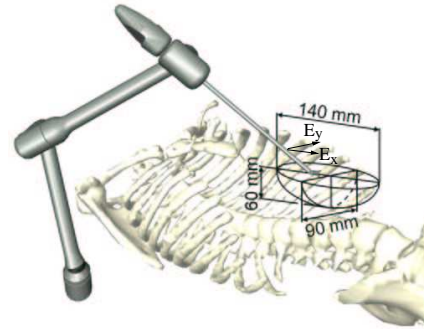
Table 1: Design parameters and constraints.



(a) Standard workspace



(b) LIMA takedown workspace



(c) Workspace considering non-actuated instruments

Figure 2: The workspaces that represent the considered surgical interventions.

3.2 Optimisation Criteria and Constraints

Defining suitable optimisation criteria and constraints is probably the most crucial factor in the optimisation process. There are many potential optimisation criteria respectively constraints, we chose the following:

- Manipulability

- Accuracy
- Geometrical considerations
- Insensitiveness of the robot setup
- Overall size of the robot

One way to handle multiple optimisation criteria is to use weighting factors and thus to combine the different criteria into a scalar performance index. This however induces the problem of finding suitable weighting factors. Another possible way is to determine the pareto-optimal front[4]. This method works fine in case of two optimisation criteria, however with three or more criteria it becomes very complex both in terms of analysis of the results and computational costs. In this work, another approach is chosen: The sole optimisation criterion is the minimisation of the overall link length $l_1 + l_2$ and thus the minimisation of the overall size of the robot. This is of great interest in an unpredictable and overcrowded environment such as the operating room. Moreover, in emergency situations the robot has to be removed manually, therefore easy manageability (light weight construction) is important. Manipulability, accuracy and geometrical considerations are added to the optimisation problem in form of constraints (Sect. 3.2.1–3.2.3). The claim for insensitiveness of the robot setup is included as described in Sect. 3.2.4. Thus the optimal setup in the chosen modelling is the one with minimal overall size that still meets all these constraints.

In the following, the considered constraints are presented and transferred into appropriate mathematical terms for actuated instruments. From this, the terms addressing non-actuated instruments can easily be derived and are thus not treated separately in this paper.

3.2.1 Manipulability

The classic formulation of manipulability based on [14] investigates the singular values of the Jacobian matrix $\mathbf{P} \in \mathbb{R}^{6 \times 8}$ in (1):

$$\mathbf{v} = \mathbf{P}\dot{\boldsymbol{\Theta}} \quad (1)$$

where $\dot{\boldsymbol{\Theta}} = [\dot{\Theta}_1, \dots, \dot{\Theta}_8]^T$ are the joint velocities and $\mathbf{v} = [v_x, v_y, v_z, \omega_x, \omega_y, \omega_z]^T$ contains the translational velocity of the instrument tip and the angular velocity of the last segment of the instrument expressed in the inertial coordinate system $[x, y, z]$ as depicted in Fig. 1. However, in the considered

case (1) cannot be used to address manipulability because it does not take into account the motion restriction due to the entry. At this point, the following kinematical constraint must be satisfied (see [9]):

$$\mathbf{C}\dot{\boldsymbol{\Theta}} = \mathbf{0}. \quad (2)$$

If the vector of joint velocities $\dot{\boldsymbol{\Theta}}$ is divided arbitrarily into a dependent part $\dot{\boldsymbol{\Theta}}_d \in \mathbb{R}^{2 \times 1}$ and an independent part $\dot{\boldsymbol{\Theta}}_i \in \mathbb{R}^{6 \times 1}$, it can be reordered as follows:

$$\dot{\boldsymbol{\Theta}} = [\dot{\boldsymbol{\Theta}}_d \dot{\boldsymbol{\Theta}}_i]^T. \quad (3)$$

The equations (1) and (2) can then be rewritten as (see [9]):

$$\mathbf{v} = \mathbf{P}_d \dot{\boldsymbol{\Theta}}_d + \mathbf{P}_i \dot{\boldsymbol{\Theta}}_i \quad \text{with} \quad \mathbf{P} = [\mathbf{P}_d \ \mathbf{P}_i] \quad (4)$$

$$\text{and} \quad \dot{\boldsymbol{\Theta}}_d = \mathbf{B}\dot{\boldsymbol{\Theta}}_i \quad \text{with} \quad \mathbf{B} \in \mathbb{R}^{2 \times 6}. \quad (5)$$

After insertion of the kinematical constraint (2), (4) has form

$$\mathbf{v} = \mathbf{P}'\dot{\boldsymbol{\Theta}}_i \quad \text{with} \quad \mathbf{P}' = \mathbf{P}_d\mathbf{B} + \mathbf{P}_i \in \mathbb{R}^{6 \times 6}, \quad (6)$$

where only 6 of the 8 joint velocities occur. Depending on which joint velocities are chosen as dependent, the Jacobian matrix \mathbf{P}' has different elements and different singular values. Therefore, it is not useful for the formulation of manipulability. A more suitable formulation is achieved if the inverse correlation is used. This can be done by solving (6) for $\dot{\boldsymbol{\Theta}}_i$ and combining the result with (5) (see [7]):

$$\dot{\boldsymbol{\Theta}} = \mathbf{D}\mathbf{v} \quad \text{with} \quad \mathbf{D} = \begin{bmatrix} \mathbf{B}\mathbf{P}'^{-1} \\ \mathbf{P}'^{-1} \end{bmatrix}. \quad (7)$$

This equation includes all joint velocities. It relates a given instrument velocity \mathbf{v} to the joint velocities $\dot{\boldsymbol{\Theta}}$ in a non-ambiguous way for every non-singular robot configuration by consideration of the kinematic constraint due to the entry point. Alternatively to the above described calculations, matrix \mathbf{D} can also be obtained by numerical differentiation. This can be done by applying difference quotients to the inverse kinematics which expresses the joint angles as function of the instrument tip position and orientation and the position of the entry point.

To define a measure for manipulability, a connection between the maximum joint velocity $\dot{\Theta}_{\max}$ and

the claimed velocities \dot{x}_{\min} and $\dot{\alpha}_{\min}$ has to be established. To do so, the matrix \mathbf{D} in (7) is split into two components

$$\mathbf{D} = [\mathbf{E} \mathbf{F}] \quad (8)$$

with

$$\mathbf{E} = \begin{bmatrix} e_{11} & e_{12} & e_{13} \\ \vdots & \vdots & \vdots \\ e_{81} & e_{82} & e_{83} \end{bmatrix}, \mathbf{F} = \begin{bmatrix} f_{11} & f_{12} & f_{13} \\ \vdots & \vdots & \vdots \\ f_{81} & f_{82} & f_{83} \end{bmatrix},$$

and (7) is rewritten:

$$\dot{\Theta} = \mathbf{E} \begin{bmatrix} v_x \\ v_y \\ v_z \end{bmatrix} + \mathbf{F} \begin{bmatrix} \omega_x \\ \omega_y \\ \omega_z \end{bmatrix}. \quad (9)$$

For each joint $i \in [1, \dots, 8]$, the maximum velocity $\dot{\Theta}_{i, \max}$ is computed by solving the optimisation problem (10):

$$\dot{\Theta}_{i, \max} = \{ |\dot{\Theta}_i(\dot{\mathbf{x}})| \xrightarrow{\text{opt}} \max \} = \{ |e_{i1}\dot{x} + e_{i2}\dot{y} + e_{i3}\dot{z} + f_{i1}\dot{\alpha}_1 + f_{i2}\dot{\alpha}_2 + f_{i3}\dot{\alpha}_3| \xrightarrow{\text{opt}} \max \} \quad (10)$$

under the constraints

$$\sqrt{v_x^2 + v_y^2 + v_z^2} - \dot{x}_{\min} \leq 0$$

$$\text{and } \sqrt{\omega_x^2 + \omega_y^2 + \omega_z^2} - \dot{\alpha}_{\min} \leq 0.$$

This is done using the Lagrange function and yields (see [7] for further details):

$$\dot{\Theta}_{i, \max} = \sqrt{e_{i1}^2 + e_{i2}^2 + e_{i3}^2} \dot{x}_{\min} + \sqrt{f_{i1}^2 + f_{i2}^2 + f_{i3}^2} \dot{\alpha}_{\min}. \quad (11)$$

Thus the maximum joint velocity

$$\dot{\Theta}_{\max} = \max(\dot{\Theta}_{i, \max}) \quad (12)$$

is determined. The constraint of manipulability is met if

$$\dot{\Theta}_{\max} < \dot{\Theta}_{\text{MAX}}. \quad (13)$$

where $\dot{\Theta}_{\text{MAX}}$ is the prescribed maximum joint velocity (see Table 1).

3.2.2 Accuracy

The following question is considered to define an accuracy measure:

How far can the instrument tip be moved at maximum with all the changes in the articular space remaining below the encoder resolution $\Delta\Theta_{\min}$?

This describes the maximum movement of the instrument tip that is not detectable by the robot control system and thus provides a worst case estimation of the positioning accuracy that can be commanded by the robot control system.

For small changes $\Delta\Theta$ and \mathbf{u} , where $\mathbf{u} = [u_x, u_y, u_z, \varphi_x, \varphi_y, \varphi_z]^T$ describes small displacements of the instrument tip and small changes in the orientation of the instrument, the following relation approximately holds:

$$\Delta\Theta = \mathbf{D}\mathbf{u}. \quad (14)$$

Since the vector \mathbf{u} contains both translational and rotational components, normalisation is applied:

$$\Delta\Theta = \tilde{\mathbf{D}}\tilde{\mathbf{u}}, \quad (15)$$

with

$$\Delta\tilde{\mathbf{u}} = \begin{bmatrix} u_x/\Delta x_{\min} \\ u_y/\Delta x_{\min} \\ u_z/\Delta x_{\min} \\ \varphi_x/\Delta\alpha_{\min} \\ \varphi_y/\Delta\alpha_{\min} \\ \varphi_z/\Delta\alpha_{\min} \end{bmatrix}, \tilde{\mathbf{D}} = [\Delta x_{\min}\mathbf{E} \quad \Delta\alpha_{\min}\mathbf{F}],$$

and Δx_{\min} , $\Delta\Theta_{\min}$ from Table 1. Thus, calculating the smallest singular value $\tilde{\sigma}_{\min}$ of $\tilde{\mathbf{D}}$ yields [7]:

$$\|\Delta\Theta\|_2 \geq \tilde{\sigma}_{\min} \|\tilde{\mathbf{u}}\|_2. \quad (16)$$

One is interested in the maximum change of one of the joint angles which is synonymous to the maximum norm $\|\Delta\Theta\|_{\infty}$ and not to the Euclidean norm as appearing in (16). Therefore, estimation (17) is used:

$$\|\Delta\Theta\|_2 \geq \|\Delta\Theta\|_{\infty} \cdot \sqrt{\dim(\Delta\Theta)}. \quad (17)$$

Claiming the instrument tip to be moved maximally by

$$u_x^2 + u_y^2 + u_z^2 \leq \Delta x_{\min}^2 \quad (18)$$

$$\text{and } \varphi_x^2 + \varphi_y^2 + \varphi_z^2 \leq \Delta\alpha_{\min}^2 \quad (19)$$

yields

$$\|\tilde{\mathbf{u}}\|_2 = \sqrt{\frac{u_x^2 + u_y^2 + u_z^2}{\Delta x_{\min}^2} + \frac{\varphi_x^2 + \varphi_y^2 + \varphi_z^2}{\Delta\alpha_{\min}^2}} \leq \sqrt{2}. \quad (20)$$

Thus, with an encoder resolution of

$$\|\Delta\Theta\|_{\infty} \geq \Delta\Theta_{\min}, \quad (21)$$

the following inequality constraint for $\tilde{\sigma}_{\min}$ is formulated:

$$\tilde{\sigma}_{\min} \geq \Delta\Theta_{\min} \sqrt{\frac{1}{2} \dim(\Delta\Theta)} \quad (22)$$

where $\Delta\Theta_{\min}$ is given in Table 1.

3.2.3 Geometrical Constraints

Besides manipulability and accuracy constraints, there are two geometrical constraints that have to be met due to design reasons. The first one addresses the length of the instrument segment remaining outside of the body l_{outside} as depicted in Fig. 3:

$$l_{\text{outside}} \geq 100 \text{ mm}. \quad (23)$$

The second geometrical constraint, also depicted in

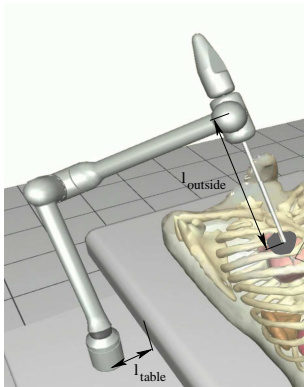


Figure 3: Geometrical constraints.

Fig. 3, restricts the distance of the robot base from the edge of the operating table:

$$l_{\text{table}} \geq 70 \text{ mm}. \quad (24)$$

3.2.4 Insensitiveness of Found Setups

Registration of the patient is – as a matter of principle – inaccurate to a certain degree. This is because of e.g. soft tissue deformation and measurement errors. Therefore, it has to be assured that the sought-after, optimised setup is robust with respect to small changes in the setup. If for example the entry point is slightly shifted, the robot still has to be able to accomplish the considered task. In order to provide insensitive setups, variations of those parameters that had been found in a preliminary study to be critical are included in the optimisation (see Fig. 2 for E_x):

- Standard workspace: shift of the entry point $E_x = -30 \text{ mm}$ and $E_x = 30 \text{ mm}$ from nominal position.
- LIMA takedown workspace: shift of the entry point $E_x = -30 \text{ mm}$ from nominal position.
- Workspace considering non-actuated instruments: shift of the entry point $E_x = -20 \text{ mm}$ and $E_x = 20 \text{ mm}$ from nominal position.

This is done by calculating the constraints not only for the nominal entry point position but also for the above mentioned variations.

3.3 Optimisation Method

Within each workspace (and its variations, see Sect. 3.2.4), a robot setup is evaluated at approximately 100 positions. Furthermore, in case of actuated instruments, 7 different orientations of the instrument tool are considered at each position: Besides the straight posture, the instrument is angled at 30° and rotated in 60° -steps around the axis defined by the entry point and the considered position (see Fig. 4). The constraints are integrated using a penalty function method.

Optimisation is carried out using genetic algorithms with a subsequent gradient-based method. Genetic algorithms are very suitable since the constraints are discontinuous. Once a setup is found that meets the constraints, gradient-based methods are faster. The optimisation is computationally quite expensive: On a standard PC (Pentium 4, 2.4 GHz), the complete optimisation cycle takes about 10 hours. Since the analysis is not time-critical, high computational costs are no problem. Nevertheless, possibilities to reduce computational

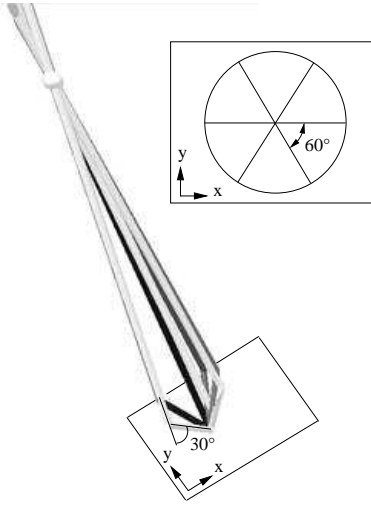


Figure 4: Orientations of the instrument tool that have been included into the optimisation procedure.

costs will be analysed in the future. This is especially of interest in more time-critical applications.

4 Results

Using the described methods, the following optimal link lengths were found:

$$l_1 = 259.5 \text{ mm} \quad \text{and} \quad l_2 = 327.4 \text{ mm}. \quad (25)$$

Figure 5 shows an analysis of insensitiveness of this setup for the standard workspace. In case of variations of the entry point E_x and E_y , a circle is drawn into the diagram to illustrate that variations of the entry point of 30 mm are tolerated by the optimised setup. Results for the other workspaces are conformable. Thus sufficient insensitiveness to compensate for registration errors can be stated.

5 Conclusion

Modified measures for manipulability and accuracy are presented to overcome the problems such as unexpected singularities or poor manipulability that were encountered with previous approaches. Furthermore, a framework for optimisation to determine the link lengths of a medical robot is described. In this context, the insensitiveness of the found robot design with respect to registration errors is

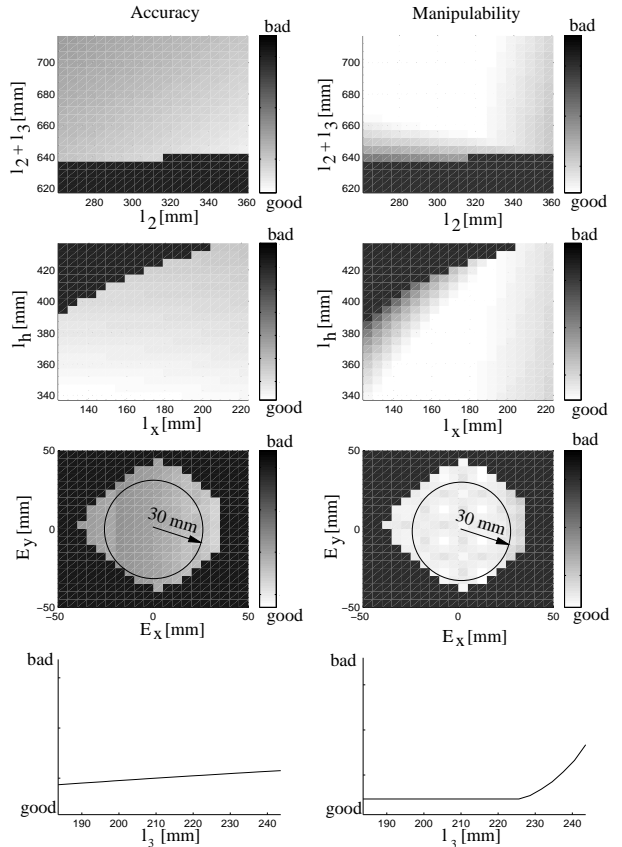


Figure 5: Analysis of sensitivity in case of the standard workspace for the found robot set-up.

a key feature. The presented methods can serve as guidelines for further robot design optimisation problems.

Work has to be done to get more precise information concerning required velocities and rotational accuracies of surgical instruments during MIS interventions. Publications in this context [10, 12, 6, 2] only cover analyses of translational accuracy.

Future work will focus on port and robot placement, based on individual patient data. The modelling will be expanded to a multi-robot setup including collision detection. Furthermore, the algorithm will be revised to reduce computational costs and thus allow for interactive applications.

References

- [1] Louaï Adhami. *An Architecture for Computer Integrated Mini-Invasive Robotic Surgery: Fo-*

- cus on Optimal Planning*. Ph.D. Thesis, Ecole des Mines de Paris, Paris, 2002.
- [2] Caroline G. L. Cao, Christine L. MacKenzie, and Shahram Payandeh. Task and Motion Analyses in Endoscopic Surgery. In *1996 ASME IMECE Conference Proceedings: 5th Annual Symposium on Haptic Interfaces for Virtual Environment and Teleoperator Systems*, Atlanta, Georgia, USA, 1996.
- [3] Adeline M. Chiu, Damini Dey, Maria Drangova, Douglas Boyd, and Terence M Peters. 3-D Image Guidance for Minimally Invasive Robotic Coronary Artery Bypass. *The Heart Surgery Forum*, 3(3):224–231, June 2000.
- [4] Kalyanmoy Deb. *Multi-Objective Optimization Using Evolutionary Algorithms*. John Wiley & Sons, June 2001.
- [5] D. Engel, W. Korb, J. Raczkowski, S. Hassfeld, and H. Woern. Location Decision for a Robot Milling Complex Trajectories in Craniofacial Surgery. In *Proceedings of the 17th International Congress and Exhibition CARS 2003*, London, UK, 2003.
- [6] Lee Hotrathinyo and Cameron Riviere. Three-Dimensional Accuracy Assessment of Eye Surgeons. In *Proc. 23rd Annual Intl. Conf. IEEE Engineering in Medicine and Biology Society*, pages 3458–3461, October 2001.
- [7] Rainer Konietschke. *Aufbauoptimierung für Roboter in medizinischen Anwendungen*. Munich University of Technology, Germany, Diploma Thesis, 2001.
- [8] Glen Lehmann, Adeline Chiu, David Gobbi, Yves Starreveld, Douglas Boyd, Maria Drangova, and Terence M. Peters. Towards dynamic planning and guidance of minimally invasive robotic cardiac bypass surgical procedures.
- [9] Tobias Ortmaier and Gerd Hirzinger. Cartesian Control Issues for Minimally Invasive Robot Surgery. In *Proc. of the IEEE/RSJ International Conference on Intelligent Robots and Systems IROS 2000*, Takamatsu, Japan, October 2000.
- [10] Cameron Riviere and Patrick Jensen. A Study of Instrument Motion in Vitreoretinal Microsurgery. In *Proceedings of the 22nd International Conference of the IEEE Engineering in Medicine and Biology Society*, July 2000.
- [11] Shaun Selha, Pierre Dupont, Robert Howe, and David Torchiana. Dexterity Optimization by Port Placement in Robot-Assisted Minimally Invasive Surgery. In *Proceedings of the 2001 SPIE International Symposium on Intelligent Systems and Advanced Manufacturing*, 2003.
- [12] Surya Singh and Cameron Riviere. Physiological Tremor Amplitude During Vitreoretinal Microsurgery. In *Proceedings of the IEEE 28th Annual Northeast Bioengineering Conference*, pages 171–172, 445 Hoes Lane, Piscataway, NJ 08855-1331, April 2002. IEEE.
- [13] Harold A. Tabaie, Jeffrey A Reinbolt, W. Peter Graper, Thomas F. Kelly, and Michael A. Connor. Endoscopic Coronary Artery Bypass Graft (ECABG) Procedure with Robotic Assistance. *The Heart Surgery Forum*, 2(4):310–317, September 1999.
- [14] Tsuneo Yoshikawa. *Foundations of Robotics: Analysis and Control*. The MIT Press, 1990.